A Dynamical Clustering Model of Brain Connectivity Inspired by the N-Body Problem

Gautam Prasad[1], Josh Burkart[2], Shantanu H. Joshi[1], Talia M. Nir[1],
Arthur W. Toga[1], and Paul M. Thompson[1]

[1] Imaging Genetics Center, Laboratory of Neuro Imaging, UCLA School of Medicine,
Los Angeles, CA, USA
[2] Department of Physics, UC Berkeley, Berkeley, CA, USA

Abstract. We present a method for studying brain connectivity by simulating a dynamical evolution of the nodes of the network. The nodes are treated as particles, and evolved under a simulated force analogous to gravitational acceleration in the well-known N-body problem. The particle nodes correspond to regions of the cortex. The locations of particles are defined as the centers of the respective regions on the cortex and their masses are proportional to each region's volume. The force of attraction is modeled on the gravitational force, and explicitly made proportional to the elements of a connectivity matrix derived from diffusion imaging data. We present experimental results of the simulation on a population of 110 subjects from the Alzheimer's Disease Neuroimaging Initiative (ADNI), consisting of healthy elderly controls, early mild cognitively impaired (eMCI), late MCI (LMCI), and Alzheimer's disease (AD) patients. Results show significant differences in the dynamic properties of connectivity networks in healthy controls, compared to eMCI as well as AD patients.

Keywords: gravity, n-body simulation, diffusion, connectivity, MRI.

1   Introduction

Modeling human brain connectivity is essential for understanding the higher level network organization of the brain [1]. Because the underlying neuronal interconnections cannot be directly observed, constructing the brain connectivity map is an inference problem. Further, there are different approaches for constructing brain networks based upon the imaging modality and the type of connectivity. For example, the neuronal fiber tracts manifest in structural anatomical connectivity [2] that is observed using diffusion-weighted imaging. Sporns et al. [1] referred to the comprehensive map of these connections as the *connectome*. However, to understand the functional organization of the brain, we can model the correlations of task activations [3] and the BOLD response from functional magnetic resonance image (fMRI). A different approach by He and Evans et al. [4] observes statistical inter-dependencies of pertinent signals in the brain. This approach is general and can also be applied to cortical thickness measures from

the brain. These types of networks also known as inference networks are useful in highlighting the compensatory processes that modulate structural measures (morphology, volume, thickness) in the brain.

At an abstract level, brain connectivity is often characterized using a connectivity matrix [5]. This connectivity matrix is an adjacency matrix that quantifies and organizes information on the connectivity between different regions of the brain. In white matter connectivity, tractography methods can assist in computing either the number or the density of extracted fibers that intersect any pair of brain regions, and provide a measure of their anatomical connectivity. The matrix of these connectivity values can also be understood as a network, which can be described using a variety of graph measures. By statistically analyzing connectivity measures from multiple subjects - of different ages or with different clinical diagnoses - it is possible to discover factors that affect the brain's connectivity network with aging and disease, and even how it is affected by our genes. Despite this, the final network representation is a topological structure, and usually does not include information on the location or size of the regions being analyzed. The size of the regions may even be regressed out using normalization to study connection density, and the relative locations of the regions are usually ignored if only the network topology is examined.

Most methods study brain connectivity as a static problem and use several sophisticated models for estimating the underlying structure. We take a different approach here and aim to model the nodal interconnectivity as a dynamical problem. This approach adapts a well known physics-based problem, the N-body simulation for dynamic modeling of particles under physical forces, imposing a dynamic structure on the nodes of the brain network. This conveniently allows one to model the nature of the interconnections by using forces proportional to the edge strengths. Traditionally, N-body simulations are used to understand dynamic systems of particles/objects under the influence of gravity. These simulations have been used by astrophysicists to understand the nonlinear formation of galaxies and related structures.

In our work, we design an N-body simulation that embodies the connectivity information of the brain to create a dynamic system of particles representing regions in the brain that interact depending on their volume and connectivity with other regions. The use of a gravitational force was motivated by the fact that, often, subnetworks with local connectivity integrate information first, and their hubs then communicate this information to other more distant centers of communication. This transfer strongly resembles the way in which N-body systems have submodules that interact and coalesce locally before interacting with other parts of the system. As such, the dynamics of the system incorporates constraints on information flow that depend on the physical proximity of the regions as well as the strength of their interaction.

Our goal is to create new measures of brain connectivity that may be useful for distinguishing disease. Our solution is a dynamic system of the locations, volumes, and fiber connectivity of a cortical segmentation, and contrasts the traditional fiber connectivity matrix with only pairwise connectivity information. Another source for our motivation is evidence of hierarchical brain organization [6].

To this end, we encoded brain measures into a gravitational N-body simulation. We used the simulation as a dynamical clustering algorithm able to produce 3D configurations of cortical segments based on connectivity rather than true physical location. We exploited similarities between information flow in brain networks and hierarchical structures formed by gravitationally interacting systems.

We present a detailed description of our connectivity based N-body simulation, outline a method for incorporating empirical connectivity data into the simulation, and describe time-dependent statistics. Additionally, we present methods for using the simulation statistics to discriminate between Alzheimer's disease and healthy control subjects in a large elderly cohort. Overall, we aim to define and simulate new models of network interaction, and observe if their properties can reveal biological differences between diagnostic groups.

2   Methods

Before designing the simulation, we assume that each subject has precomputed connectivity information that includes a parcellation of the cortex (and sometimes subcortical regions) into a set of regions with an accompanying $N \times N$ matrix characterizing their connectivity. Additionally, we also expect to know the location, size, and relationship of each region to every other region. There are several well-known approaches for partitioning the brain into a set of nodes, and for the purpose of representing the initial connectivity, our method allows any such connectivity matrix to be incorporated into our analysis.

In the following simulation design the various terms and forces are designed to restrict particle movement and bring them to a steady state reasonably quickly. We designed the particles so that their initial locations are the centroids of cortical regions and their masses are the corresponding volumes, but those initial locations are not enforced in the simulation and are quickly washed away in the early timesteps.

2.1   Gravitational N-Body Simulation

We now describe how we adapt the gravitational N-body simulation problem to brain networks. Each connectivity node corresponding to one of N regions in the cortex, is treated as a particle whose mass is proportional to the region's volume. The equations of motions for each particle i, in the traditional N-body problem are

$$\ddot{\boldsymbol{r}}_i = -G \sum_{j=1; j \neq i}^{N} \frac{m_j (\boldsymbol{r}_i - \boldsymbol{r}_j)}{|\boldsymbol{r}_i - \boldsymbol{r}_j|^3}. \tag{1}$$

where $\ddot{\boldsymbol{r}}_i$, m_i, and $\boldsymbol{r}_i$ are the acceleration, mass, and position of particle i, with G as a gravitational constant; in astrophysics, this is simply a fixed universal constant. To allow for stronger interactions between some pairs of network nodes (particles), we set the gravitational term to be the value of the connectivity matrix indexed by i and j and modified the expression so that G is replaced by

G_{ij}, which is the connectivity value for regions i and j. Intuitively, this induces a force on each particle that depends on its connectivity strength with each of the others.

In addition to the gravitational force, we include an additional attraction term, a repulsion force, and a damping force. We also include an additional attraction term to deal with "evaporation", when particles acquire too much energy and become unbound. This prevents drifting of the centroid of the N-body system. We choose the attraction term to increase as the particle separation becomes greater, as

$$-G_{ij}m_j\hat{\boldsymbol{r}}_{ij}\frac{(|\boldsymbol{r}_{ij}|/R)^b}{r_0^2}, \tag{2}$$

where $\hat{\boldsymbol{r}}_{ij}$ is the unit direction of the vector from i to j and $|\boldsymbol{r}_{ij}|$ is its norm. R is the overall size of the space and (in our neuroimaging application) is set to the largest dimension of the T1-weighted brain image and $r_0 = RN^{-1/3}$ is the inter-particle spacing. If volume of the image space is R^3, the per-particle volume is R^3/N, making $((R^3)/N)^{(1/3)} = RN^{(-1/3)}$ the initial interparticle distance. The repulsion force keeps the particles from getting too close together and prevents Equation 1 from blowing up and decreasing the timestep of the numerical solver. It is also critical for bonding of the particles in an equilibrium state. Formally, the force is

$$G_{ij}m_j\hat{\boldsymbol{r}}_{ij}\frac{d^{2a-2}}{|\boldsymbol{r}_{ij}|^{2a}}, \tag{3}$$

where $d = r_0/10$ and $a = 3$. Parameter d specifies the typical distance between particles in the equilibrium state. We chose $d = r_0/10$ to give particles sufficient initial energy to allow randomization prior to the equilibrium state's development; however, this choice is somewhat arbitrary so long as $d << r_0$. The damping force moves the system into equilibrium over time and is

$$\frac{-\boldsymbol{v}_i}{t_d}, \tag{4}$$

where $t_d = 10$ and controls the strength of the damping and time till equilibrium.

The virial theorem [7] of gravitational dynamics is

$$2\langle T \rangle + \langle V \rangle = 0, \tag{5}$$

where T is the kinetic energy of the system and V is the potential energy. It ensures that the system reaches equilibrium over time. Given this we set the typical collision time to be $t_0 = 1$ so that $r_0/v_0 = 1$ and scaled the gravity, masses, and velocity accordingly.

When combined, our modified gravity force, the attraction term, repulsion force, and damping force, specify the equations of motion for a particle as

$$\ddot{\boldsymbol{r}}_i = \sum_{j=1;j\neq i}^{N} G_{ij}\hat{\boldsymbol{r}}_{ij}m_j\left(\frac{-1}{|\boldsymbol{r}_i-\boldsymbol{r}_j|^2} + \frac{d^{2a-2}}{|\boldsymbol{r}_i-\boldsymbol{r}_j|^{2a}} - \frac{(|\boldsymbol{r}_i-\boldsymbol{r}_j|/R)^b}{r_0^2}\right) - \frac{\boldsymbol{v}_i}{t_d}, \tag{6}$$
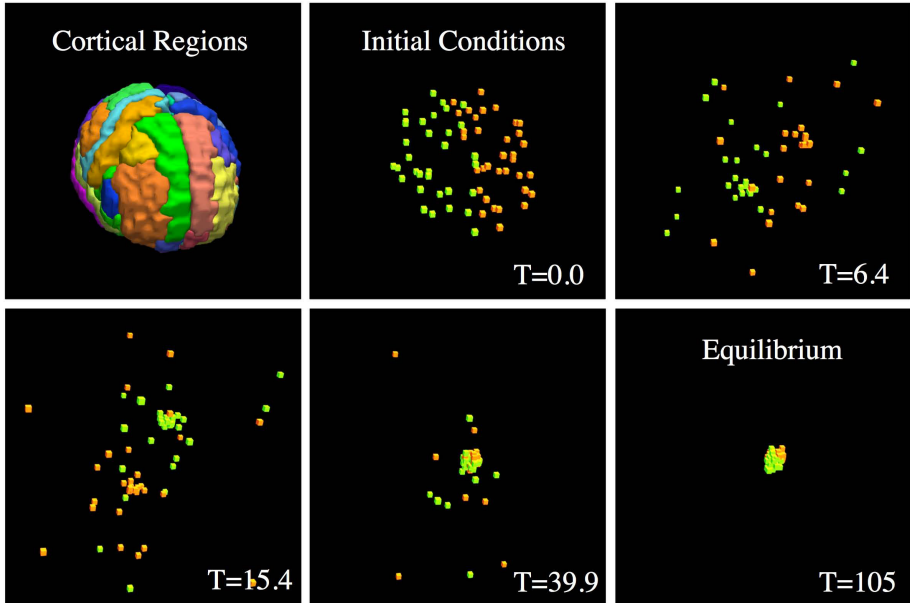
Fig. 1. We show a summary of states in our dynamical simulation of connectivity in the brain for a single subject. Each particle represents a region of the cortex and our initial conditions place a particle at the centroid of the corresponding region and assign it a mass proportional to the volume of the region. At time zero (T=0.0), we show the initial positions of all the particles coloring those in the right hemisphere green and those in the left hemisphere orange. The particles interact with each other depending on G_{ij}, which is proportional to their connectivity value and at T=6.4 and T=15.4 we can see two distinct clusters of particles in their respective hemispheres. At T=39.9 the kinetic energy of the system reduces as the system begins to reach equilibrium shown at T=105. We presented the cortical segmentation as a reminder of the initial configuration of the particles, but those locations are not enforced in the simulation and are quickly washed away in the early timesteps.

where the parameters could still be adjusted if we wanted to change how the simulation evolves. This set of equations are solved through numerical integration using the explicit Runge-Kutta (4,5) formula [8] with adaptive time steps. The simulation proceeds with the particles in each hemisphere forming clusters and ends by reaching an equilibrium configuration of the particles.

2.2 Simulation Features

We computed an N-body connectivity matrix derived from the equilibrium state. Each connectivity value represents the Euclidean distance between two particles in the final configuration with a comparison to the standard fiber connectivity matrix shown in Figure 2.

Fiber Connectivity Matrix   *N*-Body Connectivity Matrix
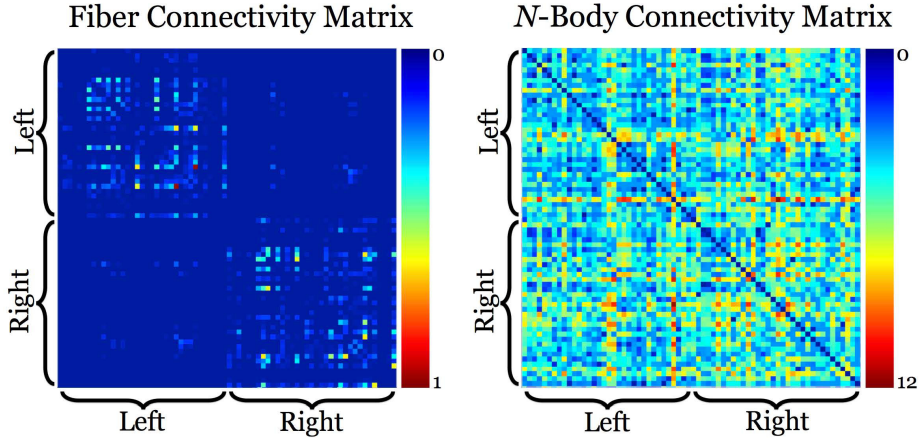
Fig. 2. We show the standard fiber connectivity matrix and our *N*-body connectivity matrix. The standard fiber connectivity matrix is an adjacency matrix where each element represents the connectivity strength between two region that is quantified by the number of fibers intersecting both regions. Our *N*-body connectivity matrix can be thought of as a nonlinear transformation of the original fiber connectivity matrix by incorporating the size and locations of the cortical regions into a dynamic system of particles.

The connectivity features we used from our method are the network measures derived from the *N*-body connectivity matrix, the time for the system to first reach equilibrium, the average speed for the centroid of the particles in addition to each particle, the total displacement of the centroid and the individual particles, and the change of distance from the initial and equilibrium states of the centroid and individual particles.

We tested the features from the simulation using two-sample *t*-tests to understand their ability to discriminate disease states in our data.

3   Experimental Results

We used a collection of 110 subjects scanned as part of the ADNI-2 [9], an extension of the ADNI project where diffusion imaging was added to the standard MRI protocol. The dataset was composed of 28 cognitively normal elderly controls (C), 56 early- and 11 late-stage MCI subjects (eMCI, LMCI), and 15 with Alzheimer's disease (AD). These subjects were scanned with a 3-Tesla GE Medical Systems scanner, which acquired both T1-weighted 3D anatomical spoiled gradient echo (SPGR) sequences (256×256 matrix; voxel size $= 1.2 \times 1.0 \times 1.0$ mm^3; TI=400 ms; TR $= 6.98$ ms; TE $= 2.85$ ms; flip angle $= 11°$), and diffusion weighted images (DWI; 256×256 matrix; voxel size: $2.7 \times 2.7 \times 2.7$ mm^3; scan time $= 9$ min). The DWIs consisted of 41 diffusion images with $b = 1000$ s/mm^2 and 5 T2-weighted

b_0 images. To process the T1-weighted images, we automatically removed extra-cerebral tissues from the images, corrected for intensity inhomogeneities using the MNI N3 tool [10], and aligned to the Colin27 template [11] with FSL FLIRT [12]. We segmented the resulting images into 34 cortical regions (in each hemisphere) using FreeSurfer [13]. These labels were then dilated with an isotropic box kernel of $5 \times 5 \times 5$ voxels to ensure they overlapped the white matter for connectivity analysis. These images were corrected for head motion and eddy current distortion in each subject by aligning the DWI images to the average b_0 image with FSL's eddy correct tool. We skull-stripped the brain using FSL and EPI-corrected with an elastic mutual information registration algorithm that aligned the DWI images to the T1-weighted scans. We generated close to 5,000 tractography fibers for each subject using a probabilistic tractography algorithm [14] and used them to compute a corresponding connectivity matrix where the connectivity value was the number of fibers that intersected a pair of regions from our dilated cortical labels.

We ran the N-body simulation for 200 timesteps (T=0-200), which provided enough time for the system to reach equilibrium, usually after 100 timesteps. In Figure 1, we step through a simulation for one subject from our experimental dataset, and visually describe the positions of the particles and their relationship to the cortical regions of our connectivity analysis. Additionally, we compared this N-body connectivity matrix to the fiber connectivity matrix that we used to define G_{ij} by computing ten different network measures [15]. These measures included mean eccentricity (ECC), global efficiency (GE), mean local efficiency (LE), mean degree (MD), transitivity, small world (SW), path length (PL), density, modularity, and the mean connectivity matrix (CM) value. We normalized the fiber connectivity matrix by the total number of fibers computed. We tested the features we computed during the simulation in two-sample t-tests comparing disease states in controls vs. AD, controls vs. LMCI, controls vs. e-MCI, and e-MCI vs. LMCI. We found the total displacement of the centroid over the simulation to be significant in discriminating controls vs. AD with a p-value of .012. We found the total displacement for one of the particles in the simulation was also significantly different comparing controls vs. AD with a p-value of

Table 1. We show the p-values from two-sample t-tests comparing features derived from the standard connectivity matrix versus our N-body connectivity matrix across a set of disease states that include 20 normal elderly controls, 56 early mild cognitively impaired (e-MCI) patients, 11 late MCI (LMCI) patients, and 15 Alzheimer's disease patients. We list the features with the lowest p-values. The features in the table are mean eccentricity (ECC), global efficiency (GE), mean connectivity matrix (CM) value, mean local efficiency (LE), and mean degree.

Test	Fiber Connectivity		N-Body Connectivity	
	Measure	p-value	Measure	p-value
Control vs. AD	Mean ECC	8.73×10^{-4}	Mean Degree	1.29×10^{-6}
Control vs. eMCI	GE	3.10×10^{-2}	Mean Degree	8.40×10^{-14}
Control vs. late-MCI	Mean CM	1.44×10^{-2}	Mean Degree	1.55×10^{-5}
eMCI vs. late-MCI	Mean LE	1.69×10^{-1}	Mean CM	1.34×10^{-4}

3.54×10^{-4} which passes the multiple comparison correction threshold at .05. In addition, one of the mean particles speeds was significant in the controls vs. AD comparison with a p-value of 1.43×10^{-5}.

4   Discussion

We presented a novel approach that simulates the inter-nodal interactions using a N-body problem. Diffusion imaging has been used before to study degenerative brain diseases, and group differences have consistently been reported for diffusion indices such as mean diffusivity and fractional anisotropy, as well as more complex network measures of anatomical connectivity. As the AD progresses, some axonal fibers are lost, and prior work has mapped the effects of this loss on brain networks, using concepts such as the k-core (a network thresholded by nodal degree) and the rich club (a property whereby the highest degree network nodes are more mutually interconnected than would be expected based on their degree). As connectivity breakdown is typical of AD and other degenerative disorders [16], new connectivity models and metrics are of interest. The N-body matrices are effective in detecting AD effects as they combine information on connectivity and volumetric atrophy, as the gravitational force depends on the size of the regions. Information transfer in the brain is impaired by each of these factors, so their use as model properties is likely to lead to metrics that differentiate AD.

A popular model of brain development was advanced by Van Essen [17] who argued that the fissures in the cortex may be formed, in part, due to the physical force of tension along long axonal fibers during embryonic development. In our formulation, the dynamics do not attempt to encode actual forces but instead resemble the flow of information to local hubs and then on to other parts of the network. Currently, the N-body problem for brain allows a free-form movement of the particles or nodes of the connectivity matrix. An interesting idea would be to constrain their displacements so that the particles are only restricted to within the brain. In the future, we plan to investigate the particle[3]-mesh method [18] that will allow us to incorporate morphological constraints along with network topology to simulate the dynamical underpinnings of human brain connectivity.

References

1. Sporns, O., Tononi, G., Kötter, R.: The human connectome: a structural description of the human brain. PLoS Computational Biology 1(4), 1–42 (2005)
2. Hagmann, P., Cammoun, L., Gigandet, X., Meuli, R., Honey, C., Wedeen, V., Sporns, O.: Mapping the structural core of human cerebral cortex. PLoS Biology 6(7), e159 (2008)
3. Friston, K.: Functional and effective connectivity in neuroimaging: a synthesis. Human Brain Mapping 2(1-2), 56–78 (2004)
4. He, Y., Chen, Z., Evans, A.: Small-world anatomical networks in the human brain revealed by cortical thickness from MRI. Cerebral Cortex 17(10), 2407–2419 (2007)

5. Biswal, B., Zerrin Yetkin, F., Haughton, V., Hyde, J.: Functional connectivity in the motor cortex of resting human brain using echo-planar MRI. Magnetic Resonance in Medicine 34(4), 537–541 (1995)
6. Zhou, C., Zemanová, L., Zamora, G., Hilgetag, C., Kurths, J.: Hierarchical organization unveiled by functional connectivity in complex brain networks. Physical Review Letters 97(23), 238103 (2006)
7. Pollard, H.: Mathematical introduction to celestial mechanics, vol. 1. Prentice-Hall (1966)
8. Dormand, J., Prince, P.: A family of embedded Runge-Kutta formulae. Journal of Computational and Applied Mathematics 6(1), 19–26 (1980)
9. Trojanowski, J., Vandeerstichele, H., Korecka, M., Clark, C., Aisen, P., Petersen, R., Blennow, K., Soares, H., Simon, A., Lewczuk, P.: Update on the biomarker core of the Alzheimer's Disease Neuroimaging Initiative subjects. Alzheimer's & Dementia: The Journal of the Alzheimer's Association 6(3), 230 (2010)
10. Sled, J., Zijdenbos, A., Evans, A.C.: A nonparametric method for automatic correction of intensity nonuniformity in MRI data. IEEE Transactions on Medical Imaging 17(1), 87–97 (1998)
11. Holmes, C., Hoge, R., Collins, L., Woods, R., Toga, A., Evans, A.: Enhancement of MR images using registration for signal averaging. Journal of Computer Assisted Tomography 22(2), 324–333 (1998)
12. Jenkinson, M., Bannister, P., Brady, M., Smith, S.: Improved optimization for the robust and accurate linear registration and motion correction of brain images. NeuroImage 17(2), 825–841 (2002)
13. Fischl, B., Van Der Kouwe, A., Destrieux, C., Halgren, E., Ségonne, F., Salat, D., Busa, E., Seidman, L., Goldstein, J., Kennedy, D.: Automatically parcellating the human cerebral cortex. Cerebral Cortex 14(1), 11–22 (2004)
14. Behrens, T., Berg, H., Jbabdi, S., Rushworth, M., Woolrich, M.: Probabilistic diffusion tractography with multiple fibre orientations: What can we gain? NeuroImage 34(1), 144–155 (2007)
15. Rubinov, M., Sporns, O.: Complex network measures of brain connectivity: uses and interpretations. NeuroImage 52(3), 1059–1069 (2010)
16. Toga, A., Thompson, P.: Connectomics sheds new light on Alzheimer's disease. Biological Psychiatry 73(5), 390–392 (2013)
17. Van Essen, D.: A tension-based theory of morphogenesis and compact wiring in the central nervous system. Nature, 313–318 (1997)
18. Eastwood, J., Hockney, R., Lawrence, D.: P3M3DP-The three-dimensional periodic particle-particle/particle-mesh program. Computer Physics Communications 19, 215–261 (1980)